Droplet ejection and sliding on a flapping film

Xi Chen, Nicole Doughramaji, Amy Rachel Betz, and Melanie M. Derby

Citation: AIP Advances **7**, 035014 (2017); doi: 10.1063/1.4979008
View online: http://dx.doi.org/10.1063/1.4979008
View Table of Contents: http://aip.scitation.org/toc/adv/7/3
Published by the American Institute of Physics

Droplet ejection and sliding on a flapping film

Xi Chen, Nicole Doughramaji, Amy Rachel Betz, and Melanie M. Derby[a]
Kansas State University, Manhattan, Kansas 66506, USA

(Received 3 October 2016; accepted 7 March 2017; published online 17 March 2017)

Water recovery and subsequent reuse are required for human consumption as well as industrial, and agriculture applications. Moist air streams, such as cooling tower plumes and fog, represent opportunities for water harvesting. In this work, we investigate a flapping mechanism to increase droplet shedding on thin, hydrophobic films for two vibrational cases (e.g., ± 9 mm and 11 Hz; ± 2 mm and 100 Hz). Two main mechanisms removed water droplets from the flapping film: vibrational-induced coalescence/sliding and droplet ejection from the surface. Vibrations mobilized droplets on the flapping film, increasing the probability of coalescence with neighboring droplets leading to faster droplet growth. Droplet departure sizes of 1–2 mm were observed for flapping films, compared to 3–4 mm on stationary films, which solely relied on gravity for droplet removal. Additionally, flapping films exhibited lower percentage area coverage by water after a few seconds. The second removal mechanism, droplet ejection was analyzed with respect to surface wave formation and inertia. Smaller droplets (e.g., 1-mm diameter) were ejected at a higher frequency which is associated with a higher acceleration. Kinetic energy of the water was the largest contributor to energy required to flap the film, and low energy inputs (i.e., 3.3 W/m^2) were possible. Additionally, self-flapping films could enable novel water collection and condensation with minimal energy input. [http://dx.doi.org/10.1063/1.4979008]

Water collection systems have been studied for dehumidification,[1–3] and fog[4–8] and dew collection.[9–13] Recovered water can be used for human consumption and agricultural purposes.[4–7] Two main mechanisms harvested water from air: droplet interception and direct condensation. Metal or plastic fog-collecting meshes intercepted droplets from the air, which were removed from screens via gravitational forces.[5–7,11] In order to be captured, a droplet must hit the mesh material, and 25% or fewer droplets were be intercepted.[8] Dew collectors tended to be radiantly cooled flat plates that condense dew primarily at night.[9–13] Environmental conditions, such as relative humidity, temperature, and wind speed affected water collection potential.[5,6,9–11] Daily water collection ranged from 1-12 L/m^2 from fog,[5–7] while waters harvests from dew were more modest.[9,13] Dew and fog water collectors were inspired by nature, including spider silk,[14,15] Namib desert beetles,[16–18] and lizards,[19] to increase water collection. Cooling tower plumes in power plants or other industrial applications represent an excellent opportunity for water collection and capture because moisture from the air can be intercepted or condensed. In a small-scale, pilot test in a 500 MW power plant, Ghosh et al.[20] recovered daily water collections of 54 L/m^2 via droplet interception using metal woven wire meshes in a cooling tower. These water collection rates in cooling tower fog were more than four times that of other fog studies.

In this study, we investigate the effects of flapping, polymer films on water droplet coalescence and shedding for water collection. Vibrations have been shown to change droplet shape and incite droplet motion on hydrophobic,[21,22] glass,[23] and polystyrene[24] surfaces as well as fibers.[25] Soft surfaces have been shown to affect the solid-liquid-air contact line and alter droplet dynamics compared to rigid surfaces.[26,27] Droplet dynamics were studied on a perfluoroalkoxy (PFA) film treated with Rain-X®coating to improve its hydrophobicity, resulting in a 107° contact angle (Figure 1a)

[a]Email: derbym@ksu.edu

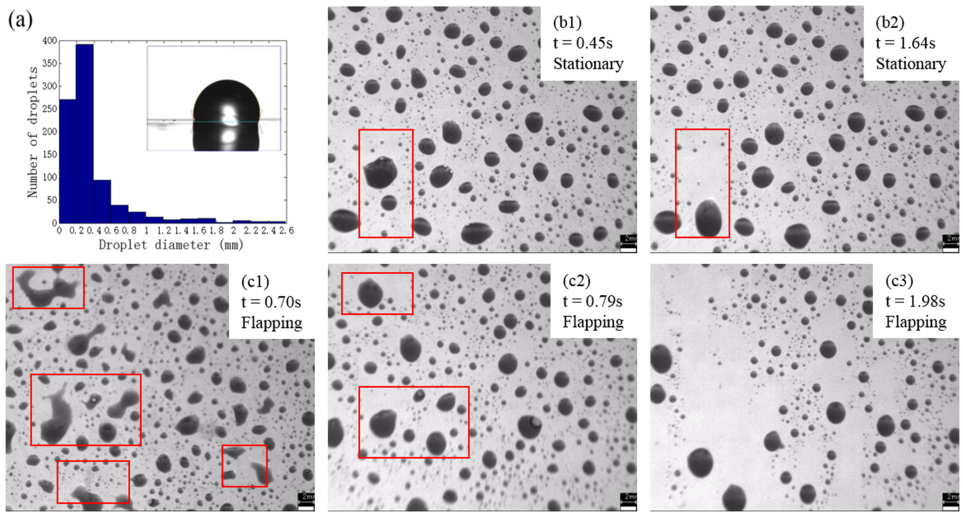

FIG. 1. (a) Histogram of droplet diameters after a single spray water droplet on hydrophobic PFA film coated with Rain-X®; droplet coalescence after one spray on a (b) stationary film and (c) film flapping at 11 Hz with a maximum displacement of ± 9 mm. (Multimedia view) [URL: http://dx.doi.org/10.1063/1.4979008.1] [URL: http://dx.doi.org/10.1063/1.4979008.2]

(Multimedia view). The film was 0.127 mm inches thick, 0.36 mm wide and 0.61 m tall. Rotation of an off-center mass provided the flapping motion for Case 1 (i.e., ± 9 mm and 11 Hz) and Case 2 (i.e., ±2mm and 100 Hz).

Water, which was dyed blue to improve visual contrast, was manually sprayed onto the film over 7 second intervals while high-speed videos were recorded from the front and side. The majority of the droplets were less than 400 μm in diameter (Figure 1a) (Multimedia view). Droplets were observed on stationary and flapping films and videos were recorded at 67 frames per second for Case 1. Videos were converted into binary images and analyzed with ImageJ to record the transient percent area covered by water. Departure sizes were recorded manually, reviewing the videos frame-by-frame using Photron FASTCAM Viewer. Droplets were removed through sliding or droplet ejection, although sliding was more prevalent in Case 1. Droplet coalescence was studied for the stationary and flapping films [Figure 1b and c (Multimedia view)] which flapped at 11 Hz. On the stationary film, the majority of droplet coalescence happened immediately after the water spray, over a period of less than 0.5 s [Figure 1b (Multimedia view)]. After this brief period of coalescence, droplets formed circular shapes and droplets larger than critical diameter slid off, absorbing small droplets in its departure path. However, on the flapping film, vibration and gravity mobilized the droplets, continually promoting coalescence both laterally and vertically over a larger area [Figure 1c (Multimedia view)], thereby increasing droplet shedding from the flapping film compared to the stationary film.

For the high displacement, low frequency Case 1, flapping reduced droplet departure diameters by 44% primarily through vibration-induced coalescence and sliding. Departure diameters of 3–4 mm were observed on the stationary film, consistent with literature,[1] compared to 1–2 mm for the flapping film [Figure 2a and b (Multimedia view)]. Departing droplets on the flapping film were smaller and rounder compared to the larger, elongated shape of gravity-driven droplets moving down the stationary film (Figure 2c) (Multimedia view). Dynamically changing advancing and receding contact angles were observed during vibrationally-driven sliding; vibrations aided droplet depinning and thus prompted droplet motion on the flapping film. Driven by increased coalescence and depinning, the flapping film rapidly shed droplets, resulting in a far lower percentage of area covered (i.e., flapping film water coverage of 6.3% compared to 13.1% on stationary film) as shown in Figure 3a. It is expected that reduced droplet departure diameters will greatly increase condensation heat transfer[28,29] and water collection rates when condensing from moist air.

In the second droplet removal mechanism, droplets were ejected perpendicularly from the flapping film. Areas with high accelerations were favorable for droplet ejection. As a first-order approximation, the instantaneous film displacement, velocity, and acceleration were estimated by the

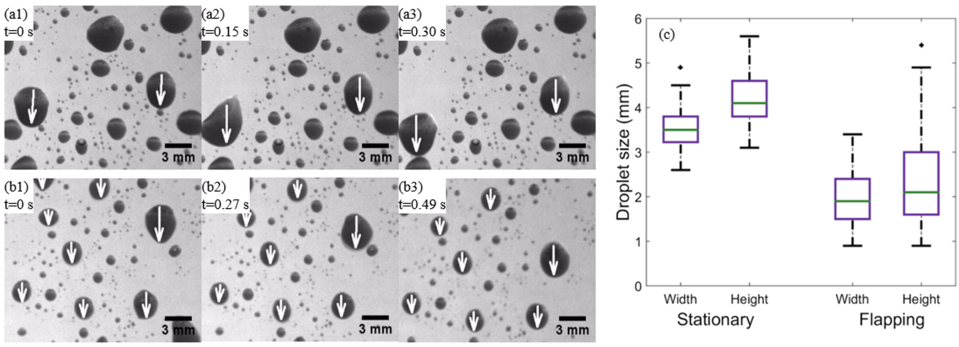

FIG. 2. Static and moving droplets on (a) stationary and (b) flapping films; (c) droplet departure diameter on both films. (Multimedia view) [URL: http://dx.doi.org/10.1063/1.4979008.3] [URL: http://dx.doi.org/10.1063/1.4979008.4]

following functions,

$$y(x,t) = B\cos\left(\frac{\pi}{2}\frac{x}{L}\right)\cos(\omega t) \tag{1}$$

$$\dot{y} = -B\omega\cos\left(\frac{\pi}{2}\frac{x}{L}\right)\sin(\omega t) \tag{2}$$

$$\ddot{y} = -B\omega^2\cos\left(\frac{\pi}{2}\frac{x}{L}\right)\cos(\omega t) \tag{3}$$

where B was maximum amplitude, x/L was non-dimensional position, ω was angular frequency, and t was time. In this formulation, the x-axis was centered on the film, and the film was clamped at positions $\pm L$. High speed videos of the flapping film captured droplet ejection [Figure 4 (Multimedia view)] for both vibrational cases. Initially, a small, stationary droplet elongated and subsequently necked, thereby demonstrating the effects of surface tension. The droplet detached from the surface with further motion of the film. Droplets removed from ejection were generally smaller than those removed from vibration-induced sweeping. Noblin et al.[21] indicated the importance of droplet surface waves on contact line oscillations under vibrations. It is hypothesized that waves generated by vibration created surface instabilities at points of maximum acceleration and displacement. As shown in Figure 4c (Multimedia view), the surface wave formed a cap-like shape and ejection depended on the balance of inertia, $F_{inertia}$, and surface tension forces, F_{st}. The excessive energy of the wave was dissipated through the subsequent elongation and necking; to prevent ejection, the surface tension force at the neck needed to be sufficiently large enough to hold the wave and prevent ejection (i.e. $F_{st} > F_{inertia}$), as shown in Figure 4a (Multimedia view). The wave was magnified by increasing the angle of the forming droplet, α, and radius R', therefore increasing inertial force. At the critical point (i.e. $F_{st} < F_{inertia}$), the inertial force surpassed surface tension and ejected the wave as droplet.

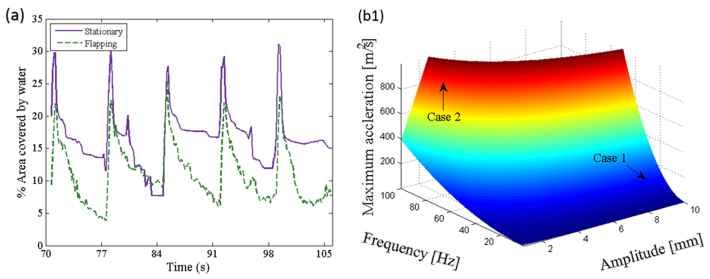

(b2)

	Case 1	Case 2
U_{max} (m/s)	0.62	1.26
a_{max} (m/s²)	43	790
D_{ej} (mm)	~2mm	~1mm
We_{ej}	0.013	0.026
Ca_{ej}	0.0077	0.016

FIG. 3. (a) Transient water area coverage on the stationary and flapping film under continuous sprays in Case 1, (b1) maximum vibrational accelerations over a range of amplitudes and frequencies and (b2) maximum plate maximum velocity, $\boldsymbol{U_{max}}$, acceleration, $\boldsymbol{a_{max}}$, ejected droplet diameter, $\boldsymbol{D_{ej}}$, and Weber and Capillary numbers of ejected droplets for vibrational Cases 1 and 2.

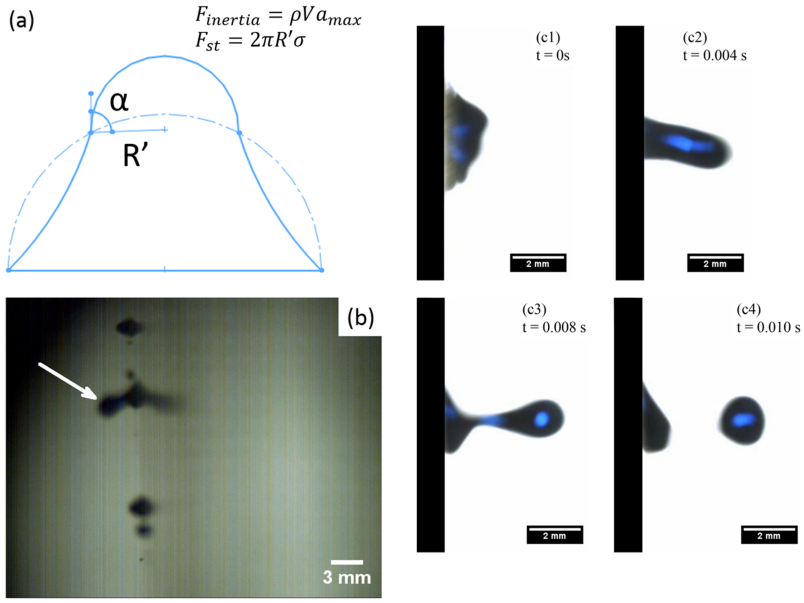

FIG. 4. (a) Diagram of droplet deformation from vibration and the inertial force at maximum acceleration and surface tension force preventing the wave from ejecting, (b) droplet ejection at ± 9-mm amplitude and 11-Hz frequency and (c) sequence of an ejecting droplet at ± 2-mm amplitude and 100 Hz. (Multimedia view) [URL: http://dx.doi.org/10.1063/1.4979008.5]

Neglecting transient start up due to the small mass of the film, the required energy input would be the energy needed to overcome the damping effects due to resistance of the air, kinetic energy of the film, and kinetic energy of the condensed water. Due to the thinness of the film, internal resistance was neglected. This air resistance was modeled as drag force, F_D, over a blunt body,

$$F_D = \frac{1}{2} C_D A_P \rho V^2 \tag{4}$$

where C_D was drag coefficient, A_P was projected area of the film, ρ was density of room temperature air, and V was air velocity. For simplification, relative air velocity was assumed to be equal to maximum centerline film velocity, 0.62 m/s and 1.26 m/s for Cases 1 and 2, respectively. The drag coefficient was estimated to be 1.9[30] and the resulting drag force was less than one Newton per cycle were small due to the low density of air and small velocity. Power was estimated as the product of force and velocity, and the energy required to overcome drag forces was low, 0.05 W and 0.65 W for Cases 1 and 2, respectively.

In addition to air resistance, the required energy input accounted for the kinetic energy of the film and water on the film. Using the maximum centerline velocity for a conservative estimate, the kinetic energy per cycle of the film multiplied by frequency, 0.21 W and 0.8 W for Cases 1 and 2, respectively. It was assumed that 0.22 kg of water resided on the film (1 kg/m^2). The kinetic energies per cycle of the water were 0.042 J and 0.18 J, and the energy required to overcome the kinetic energy of the water droplets were 0.46 W and 18 W; kinetic energy of the water was by far the dominant term. For the higher displacement, lower frequency case (e.g., ± 9 mm and 11 Hz), 0.72 W (3.3 W/m^2) were estimated, and 19 W (87 W/m^2) were estimated for the higher acceleration. Clearly accelerations have a strong impact on required energy, and in an optimal situation, the film may be able to self flap and consume minimal energy. On the flapping film, 93 droplets were shed from the 40 mm by 32 mm viewing area over a 35-second span. Departure diameters were determined from the videos and estimated departure volumes obtained. A conservative estimate, which neglects droplet removed from the swept path through coalescence with the sweeping droplet, yields a mass removal rate of 0.14 g/s for the tested film; multiplying this mass removal rate by the latent heat of vaporization returns a condensation heat transfer rate of approximately 350 W (1593 W/m^2). This analysis demonstrated that the energy required to vibrate the film and water droplets was small

compared to the energy removal rate needed to condense droplets, thereby making oscillation-driven droplet removal a viable approach.

In conclusion, droplets were rapidly shed from thin, flapping films compared to gravity-driven droplet removal on a stationary film. Droplets were removed through vibration-induced droplet coalescence or ejection from the flapping surface. This work has applications for water collection and novel flexible condensers.

The authors gratefully acknowledge the support of the National Science Foundation grant CBET-1603737, and ND would like to thank the KS-LSAMP program for support, National Science Foundation grant 1305059. Thanks also to Ian Darrah, Brandon Hulet, and Ryan Huber for assistance.

[1] J. E. Castillo, J. A. Weibel, and S. V. Garimella, International Journal of Heat and Mass Transfer **80**, 759–766 (2015).
[2] K. Hong and R. L. Webb, Journal of Heat Transfer **121**(4), 1018–1026 (1999).
[3] C. Bum-Jin, K. Sin, K. Min Chan, and M. Ahmadinejad, International Communications in Heat and Mass Transfer **31**(8), 1067–1074 (2004).
[4] R. S. Schemenauer and P. Cereceda, Journal of Applied Meteorology **31**(3), 275–290 (1992).
[5] M. J. Estrela, J. A. Valiente, D. Corell, D. Fuentes, and A. Valdecantos, Agricultural and Forest Meteorology **149**(11), 1896–1906 (2009).
[6] M. Fessehaye, S. A. Abdul-Wahab, M. J. Savage, T. Kohler, T. Gherezghiher, and H. Hurni, Renewable and Sustainable Energy Reviews **29**, 52–62 (2014).
[7] J. Olivier and C. De Rautenbach, Atmospheric Research **64**(1), 227–238 (2002).
[8] J. de Dios Rivera, Atmospheric Research **102**(3), 335–342 (2011).
[9] D. Beysens, M. Muselli, V. Nikolayev, R. Narhe, and I. Milimouk, Atmospheric Research **73**(1), 1–22 (2005).
[10] J. Maestre-Valero, V. Martinez-Alvarez, A. Baille, B. Martín-Górriz, and B. Gallego-Elvira, Journal of Hydrology **410**(1), 84–91 (2011).
[11] I. Lekouch, M. Muselli, B. Kabbachi, J. Ouazzani, I. Melnytchouk-Milimouk, and D. Beysens, Energy **36**(4), 2257–2265 (2011).
[12] G. Sharan, O. Clus, S. Singh, M. Muselli, and D. Beysens, Journal of Hydrology **405**(1), 171–181 (2011).
[13] O. Clus, P. Ortega, M. Muselli, I. Milimouk, and D. Beysens, Journal of Hydrology **361**(1), 159–171 (2008).
[14] Y. Hou, Y. Chen, Y. Xue, Y. Zheng, and L. Jiang, Langmuir **28**(10), 4737–4743 (2012).
[15] Y. Zheng, H. Bai, Z. Huang, X. Tian, F.-Q. Nie, Y. Zhao, J. Zhai, and L. Jiang, Nature **463**(7281), 640–643 (2010).
[16] B. White, A. Sarkar, and A.-M. Kietzig, Applied Surface Science **284**, 826–836 (2013).
[17] R. Garrod, L. Harris, W. Schofield, J. McGettrick, L. Ward, D. Teare, and J. Badyal, Langmuir **23**(2), 689–693 (2007).
[18] L. Zhai, M. C. Berg, F. C. Cebeci, Y. Kim, J. M. Milwid, M. F. Rubner, and R. E. Cohen, Nano Letters **6**(6), 1213–1217 (2006).
[19] W. C. Sherbrooke, Journal of Herpetology **27**, 270–275 (1993).
[20] R. Ghosh, T. K. Ray, and R. Ganguly, Energy **89**, 1018–1028 (2015).
[21] X. Noblin, A. Buguin, and F. Brochard-Wyart, The European Physical Journal E **14**(4), 395–404 (2004).
[22] L. Dong, A. Chaudhury, and M. Chaudhury, The European Physical Journal E **21**(3), 231–242 (2006).
[23] J. Whitehill, A. Neild, T. W. Ng, S. Martyn, and J. Chong, Applied Physics Letters **98**(13), 133503 (2011).
[24] E. Bormashenko, R. Pogreb, G. Whyman, Y. Bormashenko, and M. Erlich, Applied Physics Letters **90**(20), 201917 (2007).
[25] A. Bick, F. Boulogne, A. Sauret, and H. A. Stone, Applied Physics Letters **107**(18), 181604 (2015).
[26] M. Sokuler, G. n. K. Auernhammer, M. Roth, C. Liu, E. Bonacurrso, and H.-J. r. Butt, Langmuir **26**(3), 1544–1547 (2009).
[27] L. Chen and Z. Li, Physical Review E **82**(1), 016308 (2010).
[28] J. Rose, Proceedings of the Institution of Mechanical Engineers, Part A: Journal of Power and Energy **216**(2), 115–128 (2002).
[29] C. P. Migliaccio, International Journal of Heat and Mass Transfer **79**, 720–726 (2014).
[30] D. A. Kaminski and M. K. Jensen, *Introduction to Thermal and Fluids Engineering*, 1st ed. (John Wiley & Sons, Hoboken, NJ, 2005).